Molecular Crystals and Liquid Crystals

ISSN: 1542-1406 (Print) 1563-5287 (Online) Journal homepage: http://www.tandfonline.com/loi/gmcl20

Properties of Hybrid Aligned Nematic (HAN) LC Layers with Both Fixed and Unfixed Boundary Conditions

Victor V. Belyaev & Alexey S. Solomatin

To cite this article: Victor V. Belyaev & Alexey S. Solomatin (2015) Properties of Hybrid Aligned Nematic (HAN) LC Layers with Both Fixed and Unfixed Boundary Conditions, Molecular Crystals and Liquid Crystals, 613:1, 121-128, DOI: 10.1080/15421406.2015.1032087

To link to this article: http://dx.doi.org/10.1080/15421406.2015.1032087

Mol. Cryst. Liq. Cryst., Vol. 613: pp. 121–128, 2015

ISSN: 1542-1406 print/1563-5287 online
DOI: 10.1080/15421406.2015.1032087

Properties of Hybrid Aligned Nematic (HAN) LC Layers with Both Fixed and Unfixed Boundary Conditions

VICTOR V. BELYAEV[1,2,*] AND ALEXEY S. SOLOMATIN[1]

[1]Moscow Region State University, Moscow, Russia
[2]People's Friendship University of Russia

An important case of an LC layer with non-fixed LC orientation on one cell's substrate at varying LC pretilt angle on another substrate is considered. It corresponds to the de Gennes coherence length dependence on boundary conditions. Structure and optical properties of such layers are described vs. *the layer thickness, fixed pretilt angle value, light beam incidence angle. The LC elastic and dielectric properties as well as applied voltage are taken into account.*

Keywords liquid crystal alignment; coherence length; pre-tilt angle; phase retardation

1. Introduction

The configuration of hybrid aligned nematic (HAN) cells with pretilt angle on both orienting surfaces $\theta_0^{(1)}$=0, $\theta_0^{(2)}$=90° is well known [1, 2]. These cells are used to measure LC materials properties or enhance LCD performances. In [3] such geometry has been used to determine a ratio of elastic constants K_{33}/K_{11} of nematic LC by measuring the phase retardation difference of the cell. In [4–7] a few methods of determination of the pretilt angle value on each substrate of the HAN cell are described. The hybrid LC orientation can increase or decrease the viewing angles range or reduce switch time [8, 9]. In [10, 11] a symmetrical electrooptical response of the LC cell has been realized by using the HAN cell and dual-frequency steering mode. The HAN cells structure typical for both calamitic and discotic LC ($\Delta n > 0$ and $\Delta n < 0$, accordingly) is used in optical compensators [12, 13].

In [14–17] we have presented simulation results of the phase retardation difference $\Delta\Phi$ *vs.* $\theta_0^{(1)}$, $\theta_0^{(2)}$ dependences for normal and oblique incidence onto different types of the hybrid LC cells with asymmetric pretilt angles on opposite substrates. The modelling is based on the approach developed in [18–20].

There were the HAN cells with fixed boundary conditions on both cell's substrates. However there is an important case with non-fixed LC orientation on one cell's substrate at varying LC pretilt angle on another substrate. In other words there is the de Gennes coherence length *vs.* boundary conditions.

*Address correspondence to Victor V. Belyaev, Moscow Region State University, Moscow, Russia. E-mail: vic_belyaev@mail.ru

Color versions of one or more of the figures in the article can be found online at www.tandfonline.com/gmcl.

In this paper we simulate structure and optical properties of different hybrid cells.

Typical LC hybrid cells structure and properties are described in [3, 13, 14]. Optical properties of the LC cells with asymmetric boundary conditions have been considered. A method of phase retardation difference $\Delta\Phi$ value calculation for the hybrid LC cell is described in [14, 15]. Dependences of the phase retardation difference $\Delta\Phi$ on the pretilt angle values ${\theta_0}^{(1)}$ and ${\theta_0}^{(2)}$ on the opposite substrates have been calculated for the three types of the hybrid LC cells. The case of the light normal incidence and the single constant approximation (nematic LC Frank elasticity coefficients $K_{11} = K_{33}$) was considered.

In this paper we describe properties of so called one-fixed-side cells. Typical HAN cell structure is presented in Fig. 1. In [3, 14] properties of the hybrid cells with fixed LC pretilt angle on both substrates were investigated.

The LC layer in the cell is located between two internal surfaces of the substrates. In the cell reviewed one surface is covered with an orientant film and another surface is not covered with the film. The orientant-covered surface fixes specified LC director pre-tilt angle. The LC director angle on another surface is determined only by the LC elastic forces and by the applied electric field. Such case can be realized in the LC layer between two substrates situated one from another at distance d or in an LC bulk sample restricted by a plane (substrate with the fixed boundary condition) at distance d from the substrate. Another case is an LC droplet in a liquid medium. Our approach allows simulate the LC orientation penetration at different boundary tilt angles.

Under the field influence, the LC director's tilt varies. For example, for the LC with positive dielectric anisotropy, the tilt varies from the fixed value on the orienting surface to the homeotrop (vertical) state on the free surface. Certainly, for the LC with negative dielectric anisotropy, the director's tilt varies from the fixed value on the orienting surface to the planar state on the free surface.

The de Gennes parameter [21], or the coherence length, may be calculated *vs.* LC parameters and the electric field strength.

A method is developed to simulate both LC director's tilt distribution and phase retardation $\Delta\Phi$ value *vs.* fixed pretilt angle on one substrate and cell's thickness. The

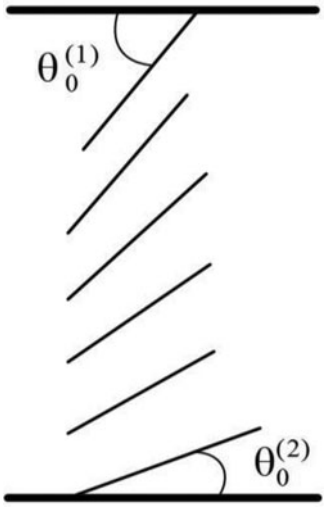

Figure 1. Hybrid LC cell structure with asymmetric pretilt angles on opposite substrates.

method is used for the LC with both positive and negative dielectrical anisotropy as well as positive and negative optical anisotropy.

In typical LC cells with static driving $0 \leq \theta_0 < \pi/2$. The phase retardation $\Delta\Phi$ for the cells with arbitrary LC director distribution is described with the expression as follows:

$$\Delta\Phi = \frac{2\pi}{\lambda}\left[\int_0^{\mathrm{L}} \frac{\mathrm{n_o n_e dz}}{(\mathrm{n_o cos^2\theta(z) + n_e sin^2\theta(z)})^{1/2}} - \mathrm{n_o L}\right]$$

where L is the cell thickness, λ is the wavelength, $\mathrm{n_o}$ and $\mathrm{n_e}$ are the refractive indices for the ordinary and extraordinary rays, accordingly, $\theta(z)$ is the LC director distribution within the cell.

A phase difference parameter $\Phi = \Delta\Phi/\Delta\Phi_{\max}$ was introduced in [19, 20]. The phase retardation difference $\Delta\Phi$ is reduced to its maximum value $\Delta\Phi_{\max} = 2\pi\Delta\mathrm{nL}/\lambda$, $\Delta\mathrm{n} = \mathrm{n_e} - \mathrm{n_o}$ is the LC birefringence. The case of $\Delta\Phi_{\max}$ is realized for the cells with the LC planar alignment ($\theta_0{}^{(1)} = \theta_0{}^{(2)} = 0$). As in [19, 20], single-constant approach was used. Two Frank elasticity constants for nematic LC are equal: K_{11}=K_{33}. The director lays in the plane perpendicular to the cell's surface.

2. Methods

2.1. LC Director Orientation

The Freederickx effect in magnet field, in the case of the planar nematic cell and the field perpendicular to the surface, may be described as follows [22, 23]:

$$\frac{d}{dz}\left[(K_{11}\cos^2\theta + K_{33}\sin^2\theta)\left(\frac{d\theta}{dz}\right)^2 + \chi_\alpha H^2 \sin^2\theta\right] = 0$$

The expression may be transformed to a view:

$$\left\{2\left(\frac{d^2\theta}{dz^2}\right)\left(K_{11}\cos^2\theta + K_{33}\sin^2\theta\right) + 2\left(\frac{d\theta}{dz}\right)^2((K_{33} - K_{11})\sin\theta\cos\theta) + 2\chi_\alpha H^2 \sin\theta\cos\theta\right\}\left(\frac{d\theta}{dz}\right) = 0$$

If $\frac{d\theta}{dz} = 0$, then the LC cell has a constant director tilt. It is valid without the field, although the director's distribution cannot be linear in this case at high field strength.

If ($\mathrm{K_{11}} = \mathrm{K_{33}}$), we may conclude:

$$\left(\frac{d^2\theta}{dz^2}\right)K_{11} + \chi_\alpha H^2 \sin\theta\cos\theta = 0$$

Then $\left(\frac{d^2\theta}{dz^2}\right) = -\frac{\chi_\alpha H^2 \sin\theta\cos\theta}{K_{11}}$ and $\left(\frac{d\theta}{dz}\right) = \frac{\chi_\alpha H^2\cos^2\theta}{2K_{11}}$ or $\left(\frac{d\theta}{dz}\right) = -\frac{\chi_\alpha H^2\sin^2\theta}{2K_{11}}$.

For the electric field and the LC with positive dielectric anisotropy this expression can be transformed to a view:

$$\frac{d\theta}{dz} = M\cos^2\theta$$

and in the case of negative dielectric anisotropy:

$$\frac{d\theta}{dz} = M\left(-\sin^2\theta\right).$$

Where $M = \frac{\varepsilon_0 \Delta\varepsilon E^2}{2K_{11}}$ is a parameter, $E = U/d$ is electric field strength, d is the cell's thickness.

2.2. Optical Properties

Let us review a case of oblique incidence of a polarized light beam onto the HAN cell (Fig. 2). The case of parameter Φ calculation for the case of both normal and oblique light incidence onto typical HAN cells with different pretilt angles has been considered in [14, 15]. Light incidence will be considered by the method, described in these references.

The angle β is the incidence angle, and the plane *12* (lines *1* and *2* form the direct angle) is parallel to the LC director plane *xz*. Therefore the light wave E-vector is perpendicular to these planes. This geometry is equivalent to the normal incidence onto the hybrid cell (Fig.1) with pretilt angles on the opposite substrates equal to $\gamma^{(1)}=\theta_0{}^{(1)}+\beta$ and $\gamma^{(2)}=\theta_0{}^{(2)}+\beta$ accordingly. The equivalent cell's thickness is increased in this case by a factor of $1/\cos\beta$.

The LC cell's layer is divided into a lot of thin layers. Every thin layer has the constant director tilt angle and contributions of the layers into both extraordinary and ordinary light beams would be added.

The director's tilt angle distribution is linear. So, every thin layer's director tilt increases for the same small angle.

3. Modeling

3.1. LC Director's Tilt Distribution in the Case of LC with Both Negative and Positive Dielectric Anisotropy

Under the field influence, the director's tilt varies. For the LC with negative dielectric anisotropy, it changes from the fixed value on the orienting surface to the planar state on the opposite surface. For the LC with positive dielectric anisotropy, it changes from the fixed value on the orienting surface to the vertical orientation on another surface.

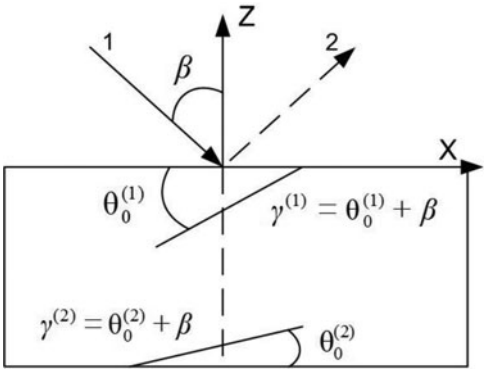

Figure 2. Light beam incidence onto a HAN cell with different boundary conditions.

While the field strength increases, the coherence length decreases.

Figure 3a shows us the director tilt distribution *vs.* the LC layer thickness ($\Delta\varepsilon > 0$) and pre-tilt angle on the surface covered with the orientant at M = 0.1 (low electric field strength). Figure 3b shows us director tilt distribution *vs*. LC layer thickness for different fixed pre-tilt angles. Figure 3c presents tilt angle value at distance *d* from orienting surface *vs.* LC layer thickness and pre-tilt angle on the surface covered with the orientant for different *d* values.

The same dependences for the LC with $\Delta\varepsilon > 0$ can be obtained by replacements $\theta_2(\Delta\varepsilon < 0)\pi/2 \leftrightarrow \theta_2(\Delta\varepsilon > 0), \theta_1(\Delta\varepsilon < 0)\pi/2 \leftrightarrow \theta_1(\Delta\varepsilon > 0)$. Data for the director tilt distribution calculated at other M values (from 0.1 to 0.8) and for the LC with positive dielectric anisotropy are presented in [24].

The LC tilt change from its fixed value at the substrate is growing up with an increase of the fixed pretilt angle and reducing with an increase of the layer thickness.

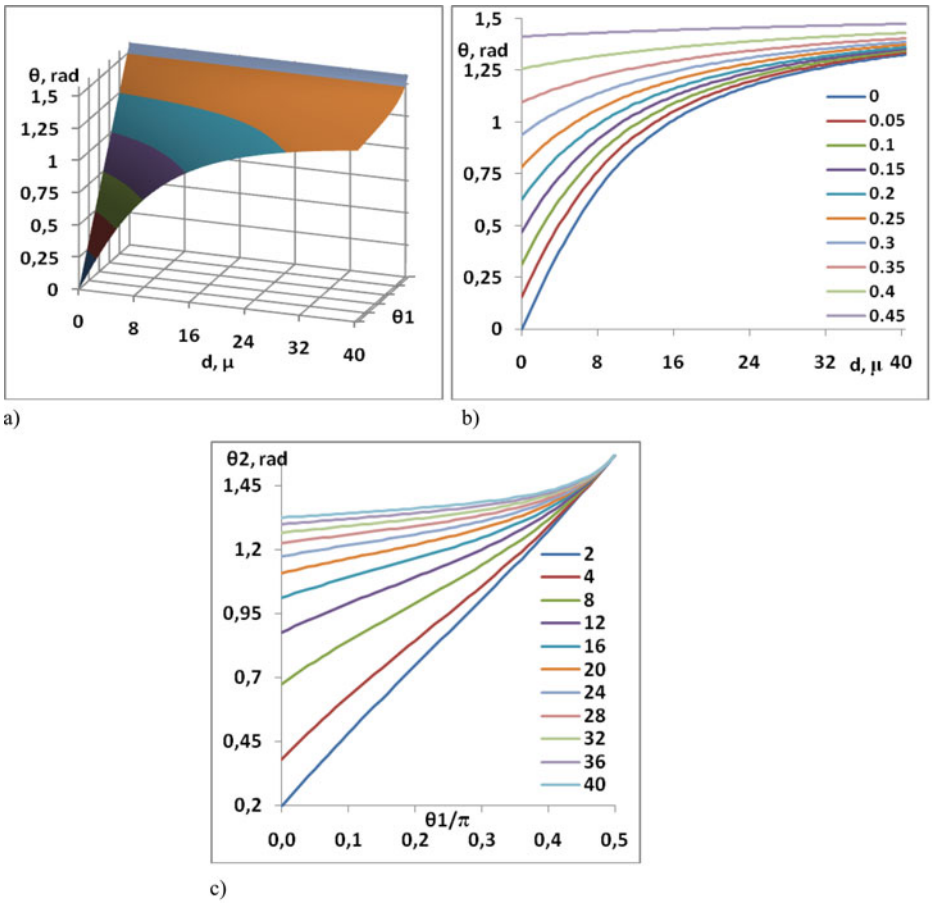

Figure 3. a) 3D view of the LC director tilt distribution *vs.* the LC layer thickness and pre-tilt angle on the surface covered with the orientant; b) director tilt distribution *vs*. LC layer thickness for different fixed pre-tilt angles; c) tilt angle value at distance *d* from orienting surface *vs.* LC layer thickness and pre-tilt angle on the surface covered with the orientant for different *d* values.
Parameter M = 0.1 (low electric field strength).

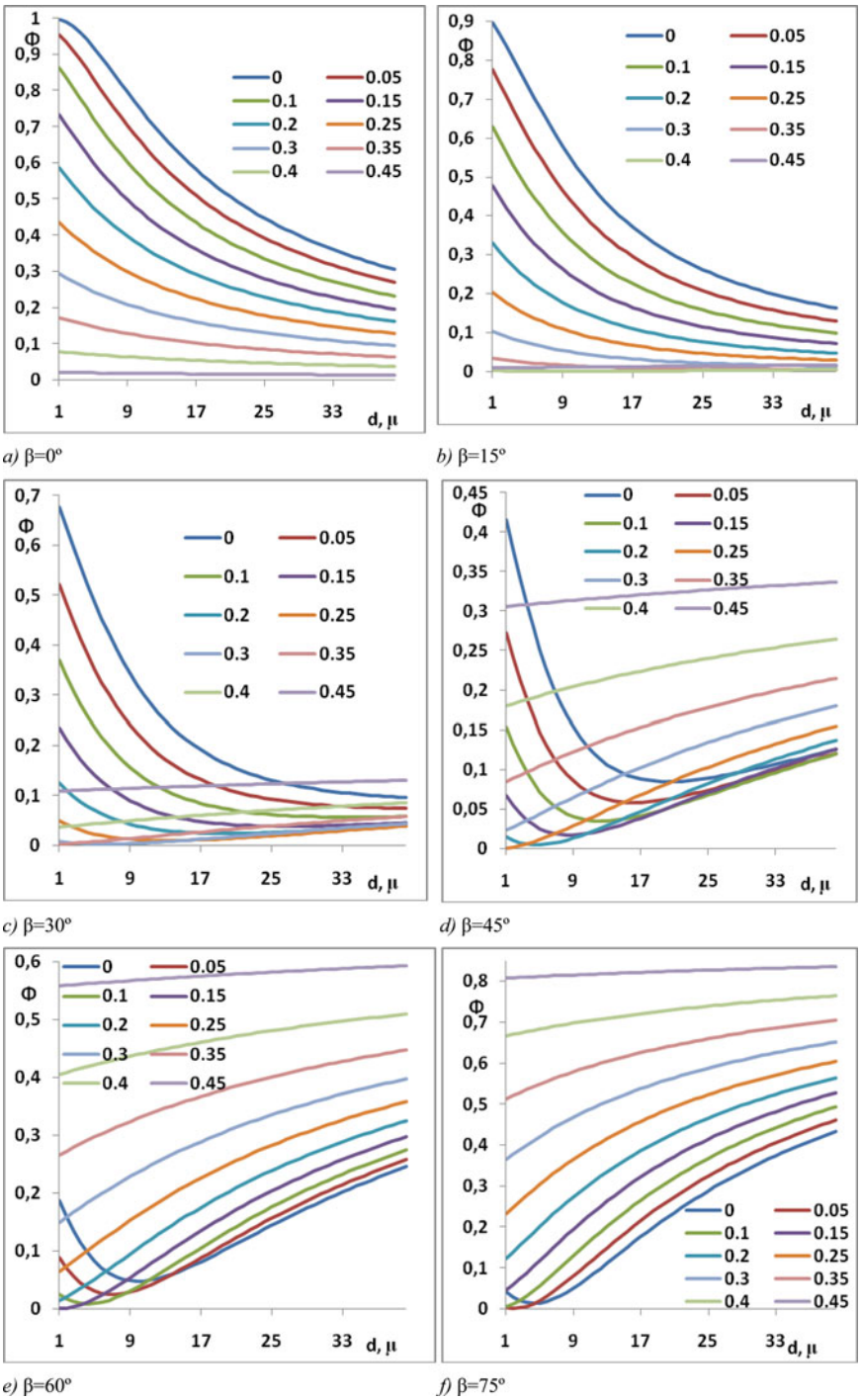

Figure 4. Phase retardation parameter Φ value for the one-side hybrid LC cell *vs.* the cell's thickness at different values of both fixed pretilt angle from 0 to 90° and incidence angle in the range from 0 to 75°.

3.2. Optical Properties in the Case of Both Positive and Negative Dielectric Anisotropy

Figure 4 shows us the phase retardation parameter Φ value for the one-fixed-side cells *vs.* the cell's thickness at different values of both fixed pretilt angle from 0 to 90° and incidence angle in the range from 0 to 75°. Parameter M is equal to 0.1 and refraction indices $n_o = 1.5$, $n_e = 1.7$; $\Delta\varepsilon > 0$. The same dependences for the LC with $\Delta\varepsilon > 0$ can be obtained by replacements ß($\Delta\varepsilon < 0$) $= \pi/2 -$ ß($\Delta\varepsilon > 0$).

Let's analyze the $\Phi(\theta_0, z)$ dependences. As shown on Fig. 4, differences between the cases of light incidence are the most significance, if $\beta = 45°$. As it seems, both the incidence cases are the same if $\beta = 0°$ or $\beta = 90°$.

Let us consider the case of oblique incidence in more details. The magnitude of the Φ variation changes in different ranges while the angle β rises at different fixed pretilt angle θ_0. For planar orientation ($\theta_0 = 0$) the Φ magnitude reduces from the unit to 0.06 when the incidence angle increases from 0 to 75°. For the vertical orientation ($\theta_0 \sim \pi/2$) the Φ behavior is more sophisticated. If at normal incidence the Φ value increases from zero at zero thickness to 0.7 at $d = 40$ μm, such dependence becomes reducing from 0.8 to 0.12 in the same thickness range at almost sliding light beam ($\beta = 75°$). The $\Phi(\theta_0, z)$ dependences have minima in the incidence angle β range from 30° to 60°. Such behavior is owing to change of the light beam propagation direction in relation to the average LC orientation direction inside the HAN cells. If the light beam direction coincides with the predominant LC orientation in the cell the HAN cell becomes mostly like the vertically aligned cell and the Φ has its minimum value.

4. Conclusions

- New type of the LC layer (so called one-fixed-side cells) with both fixed and unfixed LC orientation on opposite surfaces is reviewed. Such layers can exist in the hybrid nematic cells with weak boundary condition on one substrate or in the LC bulk at a definite distance from the surface with fixed boundary orientation.
- New method of coherence length evaluation and control is proposed with using a set of LC cell's parameters variation. Such set comprises pre-tilt angle, cell's thickness and also a field strength; dielectric and elastic LC properties must be taken into consideration too.
- The one-fixed-side cell optic properties control and measurement method is proposed, using cell's orientation parameters varying, as above.

Funding

This work was supported by Russian Foundation for Basic Researches, grant #14-07-00574_a.

References

[1] Matsumoto, S., Kawamoto, M., & Mizunoya, K. (1976). *J. Appl. Phys.*, *47*, 3842–3845.
[2] Lu, Y.-Q., Liang, X., Wu, Y.-H., Du, F., & Wu, S.-T. (2004). *Appl. Phys. Lett.*, *85*, 3354–3356.
[3] Beresnev, G. A., Chigrinov, V. G., & Grebenkin, M. F. (1982). *Crystallography Reports*, *27*, 1019–1021.
[4] Zheng, G., & Zhang, Z. (2010). *Molecular Crystals and Liquid Crystals*, *528*, 103–112.
[5] Wang, S.-Y., Wu, H.-M., & Yang, K.-H. (2013). *Applied Optics*, *52*, 5106–5111.

[6] Baek, J.-I., Kim, K.-H., Kim, J. C., & Yoon, T.-H. (2009). *Molecular Crystals and Liquid Crystals*, *498*, 103.
[7] Jeong, E., Lim, Y. J., Chin, M. H., Kim, J. H., Lee, S. H., Ji, S. H., Lee, G.-D., Park, K. H., Choi, H. C., & Ahn, B. C. (2008). *Applied Physics Letters*, *92*, 261102.
[8] Ryu, J. W., Lim, Y. J., Jeong, Y. H., Kim, K., Lee, G.-D., & Lee, S. H. (2007). *Japanese Journal of Applied Physics*, *46*, 5951.
[9] Kim, W. C., Jeong, Y. H., & Lee, S. H. (2004). *Japanese Journal of Applied Physics*, *43*, 637.
[10] Konshina, E. A., Vakulin, D. A., Ivanova, N. L., Gavrish, E. O., & Vasiliev, V. N. (2012). *Technical Physics*, *57*, 644–648.
[11] Ivanov, A. V., Vakulin, D. A., & Konshina, E. A. (2014). *Journal of Optical Technology*, *81*, 130–134.
[12] Bos, P. (2002). Liquid crystal modes for wide viewing angle, *Applications Tutorial, SID*, Boston, MA, May 21–23.
[13] Yeh, P. (2006). LC Modes for Various Display Applications, *SID '06 Symposium*, Applications Tutorial.
[14] Belyaev, V. V., Solomatin, A. S., Kurilov, A. D., Chausov, D. N., Mazaeva, V. G., Shoshin, V. M., & Bobylev, Y. P. (2014). *Applied Optics.*, *53*, H51.
[15] Belyaev, V. V., Solomatin, A. S., & Chausov, D. N. (2014). *Molecular Crystals and Liquid Crystals*, *596*, 22.
[16] Belyaev, V. V., Solomatin, A. S., & Chausov, D. N. (2013). *SID'13 Digest*, pp.1422–1425.
[17] Belyaev, V. V., Solomatin, A. S., Kurilov, A. D., Chausov, D. N., Mazaeva, V. G., Shoshin, V. M., & Bobylev, Y. P., (2014). *SID 2014 Digest of Technical Papers*, pp. 1445–1448.
[18] Belyaev, V. V., Solomatin, A. S., Chausov, D. N., & Gorbunov, A. A. (2012), *SID'12 Digest*, pp. 1422–1425.
[19] Belyaev, V., Solomatin, A., & Chausov, D. (2013). *Optics Express*, *21*, 4244–4249.
[20] Belyaev, V. V., Solomatin, A. S., & Chausov, D. N. (2013). *Applied Optics*, *52*, 3012–3019.
[21] de Gennes, P. G. (1974). *Physics of Liquid Crystals*. Clarendon Press. Oxford.
[22] Blinov, L. (2010). *Structure and Properties of Liquid Crystals*. Springer.
[23] Chandrasekhar, S. (1993). *Liquid Crystals.* 2nd Edition. Cambridge University Press.
[24] Belyaev, V. V., & Solomatin, A. S. (2014). *Liquid Crystals and Their Application*, *14*, (2), 4.